J. Appl. Comput. Mech., 7(4) (2021) 1973–1986
DOI: 10.22055/JACM.2020.33456.2228

ISSN: 2383-4536
jacm.scu.ac.ir

Shahid Chamran University of Ahvaz

Journal of Applied and Computational Mechanics

Research Paper

Magneto-bio-thermal Convection in Rotating Nanoliquid containing Gyrotactic Microorganism

Meenakshi Khurana[1], Puneet Rana[2,3], Sangeet Srivastava[1], Sanjay Yadav[1]

[1] Department of Mathematics, The NorthCap University, Sector 23A, Gurugram, Haryana 122017, India

[2] School of Mathematical Sciences, College of Science and Technology, Wenzhou Kean University, Wenzhou 325060, China

[3] Department of Mathematics, Jaypee Institute of Information Technology, A-10, Sector 62, Noida 201309, India

Received May 02 2020; Revised June 22 2020; Accepted for publication July 13 2020.
Corresponding author: P. Rana (puneetranaiitr@gmail.com; prana@kean.edu)

Abstract. The magneto-convection influenced by a gyrotactic behavior of algal suspensions along with rotation in the nanoliquid layer is investigated. Linear theory based on normal mode analysis is used to find out the inquisitive results of the problem for rigid-free and rigid-rigid boundaries. Both Galerkin-method (Number of terms (N) > 6) and shooting method (by taking forcing condition) are utilized to find the critical value of the Rayleigh number (both thermal and bio) in case of non-oscillatory stability. Both thermal and bio Rayleigh numbers are dependent on each other, thus advance or delay the convection. Rotation and magnetic field slow down the convective motion of microorganisms across the layer and destabilizes the system.

Keywords: Microorganism, Bio-convection, Nanofluid, Rayleigh number, Galerkin Method, Shooting method.

1. Introduction

Bio-convection is a macroscopic convection induced in water due to density stratification by up swimming of an enormous number of self-propelled motile microorganisms like algae and bacteria. A nanofluid bio-convection is a combination of nano-liquid with bio-convection which is a new area of research among researchers for micro and nano-fluidic devices. As, we know that gyrotactic micro-organisms are 3 to 5 percent denser than water, so, these always move upwards in the liquid balancing torques due to gravity and shear flow. Thus a pattern of Bénard cells, similar to the zig-zag motion of nanoparticles in the base fluid, is developed in the layer due to their mean swimming velocity, swimming modes and rotational diffusion in the liquid. Moreover, microorganisms help to form a stable suspension of nano-liquid preventing nanoparticles from gravity settling, agglomeration, and abrasion in fluid walls. So, it has potential to enhance mass transfer in micro-volumes [1] which has struck in the mind of researchers for the design of micro-systems like micro-channels based cooling systems [2], micro channel heat sink [3], cooling of microchips [4], micro reactors [5] and micro heat pipes [6]. Also, they have many applications in bio-micro-systems like nano-drug delivery [7] and enzyme bio-sensors [8].

Definite spatial bio convection patterns like Rayleigh-Taylor instability are first observed in 1974 in their experiments by Plesset and Winet [9]. Then in 1975, a model has been presented by Childress et al. [10] for combined motion and creation of patterns in the suspensions of negatively geotactic microorganisms. After that, a continuous progress by many authors [11]–[18] in the stability analysis and numerical investigation in bio convection patterns caused by gyrotactic micro-organisms is made. The stability analysis of bio-convection in a suspension of gyrotactic micro-organisms in small solid particles is done by Kuznetsov and Avramenko [19], Kuznetsov and Geng [20], Geng and Kuznetsov [21]. These authors have investigated that small particles (nanoparticles-with negligible settling velocity, very large particles-with negligible diffusivity, very heavy particles-with very large settling velocity) do not have much impact on bioconvection as they simply settle down at the bottom but the particles with optimal size and density effectively delay the bioconvection in the fluid layer. Kuznetsov and Avramenko [22] have given the analytical expression for the critical value of permeability of a porous medium by linear stability utilizing algal suspensions and established that if the permeability is greater than its critical value then the suspension of micro-organisms is unstable and otherwise stable. Also, Kuznetsov [23, 24] conferred a bio-convection problem in a nanofluid layer containing gyrotactic microorganisms and presented the analytical expressions for oscillatory and non-oscillatory Rayleigh number for RR and RF boundary conditions and have shown that up-swimming micro-organisms destabilizes the onset of bio-convection in the layer.

Bioconvective flows in nano-liquids along with magnetic field and rotation present an interesting fluid dynamic problem. Both magnetic field and rotation work as a good controller to bioconvective nanofluid flows. It has numerous applications in micro-electro mechanical systems used in medicine, design of micro fluidic devices used in treatment of cancer and some arterial diseases and reduction of blood through surgeries, in rotating disk bio-reactors in chemical engineering processes for chromatography, oil modeling, materials processing systems with magnetic field control, in microbial fuel cell coatings and in the synthesis of nano-bio polymers [25-28]. A lot of numerical investigations have been carried out in bioconvective layer on all these

Published online: March 10 2021

parameters altogether but few analytical results have been established yet. Khan et al. [29, 30] have focused on three dimensional swirling flows with swimming micro-organisms and discussed the effect of AAE (Arrhenius Activation energy) on the start of binary chemical reaction both analytically and numerically. This AAE with nanofluid and microorganisms has countless applications in magneto-hydrodynamics, environmental science, micro-biology, pharmaceutical and oil industries. Atif et al. [31] have presented magneto-hydrodynamics stratified micro polar convective fluid flow containing nanoparticles and micro-organisms. They have applied similarity transformation and shooting method to solve the PDE's numerically to find the effect of various parameters on velocity, temperature, nanoparticle concentration and motile micro-organisms. Khan et al. [32] have reviewed the bio-convection based analysis involving two stretchable rotating disks with entropy generation and solved the problem by HAM (Homotopy Analysis Method) and established that velocity decreases with magnetic field and stretching parameter, temperature increases with Brownian motion and thermophoresis, nanoparticle volume fraction decreases with Lewis number and diffusivity ratio and microorganisms increase with Lewis number and Peclet number. Also, numerical investigations in bio-convection nanofluid flows with impact of external magnetic field in rotating system have been made by Saleen et al. [33], Raju and Sandeep [34] and Tarakaramu and Narayana [35].

In this paper, we presented a linear theory to scrutinize the bio-convection in a fluid layer containing nanoparticles and gyrotactic micro-organisms along with magnetic field and rotation. Both RR and RF boundaries have been considered and not only analytical but also numerical results have been validated with other researchers. The combined effect of all these parameters on the stability analysis of fluid layer along with bio-microorganisms and nanoparticles has not been studied yet to the best of author's knowledge.

2. Governing Equations

A nanoliquid containing gyrotactic microorganisms is considered under the combined influence of magnetic field H_0 (effective due to electrical conducting nature of ionized water) as well as rotation with constant angular velocity $\Omega^* = (0,0,\Omega^*)$ with the assumption that low concentration of nanoparticles in the nano-liquid does not affect the swimming speed and direction of microorganisms (see Fig 1.). The final controlling equations based on ref. [11-14] and with new findings, Siddheshwar and Kanchana [36] and Wakif et al. [37] are written as

$$\nabla.\mathbf{v}^* = 0 \tag{1}$$

$$\rho_{nl}\left(\frac{\partial \mathbf{v}^*}{\partial t} + \mathbf{v}^*.\nabla^*\mathbf{v}^*\right) + \sigma_{nl}(\mu_m)_{nl}^{\ 2} H_0^{\ 2}\mathbf{v}^* - \frac{2}{\delta}\left(\mathbf{v}^* \times \Omega^*\right) = -\nabla^* p^* + \mu_{nl}\nabla^{*2}\mathbf{v}^* - \left[1 - \beta_{nl}\left(T^* - T_0^*\right) + \beta_\phi\left(\phi^* - \phi_0^*\right)\right]\rho_{nl} g\hat{\mathbf{k}} - n^*\theta\Delta\rho_m g\hat{\mathbf{k}} \tag{2}$$

$$(\rho c)_{nl}\left(\frac{\partial T^*}{\partial t^*} + \left(\mathbf{v}^*.\nabla^*\right)T^*\right) = k_{nl}\nabla^{*2}T^* + (\rho c)_{np}\left(D_B\nabla^*\phi^*.\nabla^*T^* + D_T\frac{\nabla^*T^*.\nabla^*T^*}{T^*}\right) \tag{3}$$

$$\frac{\partial \phi^*}{\partial t^*} + \left(\mathbf{v}^*.\nabla^*\right)\phi^* = \nabla^*.\left(D_B\nabla^*\phi^* + \frac{D_T}{T^*}\nabla^*T^*\right) \tag{4}$$

$$\frac{\partial n^*}{\partial t^*} = -\nabla^*.j^* \tag{5}$$

$$j^* = n^*\mathbf{v}^* + n^* W_c\hat{\mathbf{p}} - D_m\nabla^* n^* \tag{6}$$

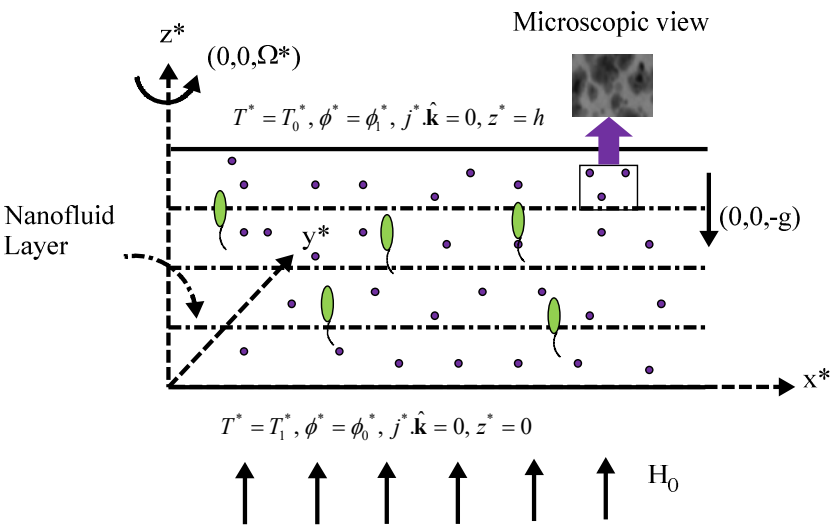

Fig. 1. Schematic Diagram of Physical Problem

with boundary conditions

$$T^* = T_1^*, \phi^* = \phi_0^*, j^*.\hat{\mathbf{k}} = 0, z^* = 0 \tag{7}$$

$$T^* = T_0^*, \phi^* = \phi_1^*, j^*.\hat{\mathbf{k}} = 0, z^* = h \tag{8}$$

j^* is the total flux of microorganisms having vector $W_c\hat{\mathbf{p}}$ which refers to average swimming velocity w.r.t. nanoliquid as suggested by Pedley et al. [10] and Hill et al. [12] and D_m is the diffusivity of microorganisms. Here the correlation of $\rho_{nl}, \rho_{np}, \sigma_{nl}, (\mu_m)_{nl}, \beta_{nl}, \beta_\phi, k_{bl}, k_{nl}, (\rho c)_{bl}, (\rho c)_{nl} (\rho c)_{np}$ has been taken from the ref. [36], [37] where subscripts bl, nl, np represent the base liquid, nanoliquid and nanoparticles respectively. Introducing the following dimensionless variables

$$(x,y,z) = (x^*, y^*, z^*)/h, (u,v,w) = (u^*, v^*, w^*)h/\alpha_{bl}, t = \frac{t^*\alpha_{bl}}{h^2}, \Omega^* = \frac{d^2}{\alpha_{bl}}\Omega, p = \frac{h^2 p^*}{\mu_{nl}\alpha_{bl}}, T = \frac{T^* - T_0^*}{T_1^* - T_0^*}, \phi = \frac{\phi^* - \phi_0^*}{\phi_1^* - \phi_0^*}, n = n^*\theta \tag{9}$$

The dimensionless form of Eqs. (1)-(5) becomes

$$\frac{1}{\Pr}\left(\frac{\partial \mathbf{v}}{\partial t} + \mathbf{v}.\nabla\mathbf{v}\right) + Q\mathbf{v} - \sqrt{Ta}\left(\mathbf{v}\times\hat{\mathbf{k}}\right) + \nabla p = \nabla^2\mathbf{v} + (RaT - Rn\phi)\hat{\mathbf{k}} - \frac{Rb}{Lbc}n\hat{\mathbf{k}} \tag{10}$$

$$\frac{\partial T}{\partial t} + \mathbf{v}.\nabla T = \nabla^2 T + \frac{N_B}{Le}\nabla T.(\nabla\phi + N_A\nabla T) \tag{11}$$

$$\frac{\partial \phi}{\partial t} + \mathbf{v}.\nabla\phi = \frac{1}{Le}\nabla^2\phi + \frac{N_A}{Le}\nabla^2 T \tag{12}$$

$$\frac{\partial n}{\partial t} = -\nabla.\left[n\left(\mathbf{v} + \frac{Pe}{Lb}\hat{\mathbf{p}}\right) - \frac{1}{Lb}\nabla n\right] \tag{13}$$

with boundary conditions

$$T = 1, \phi = 0, nPe = \frac{dn}{dz}, z = 0 \tag{14}$$

$$T = 0, \phi = 1, nPe = \frac{dn}{dz}, z = 1 \tag{15}$$

The dimensionless parameters which have usual meaning, used in the Eqs. (10)-(13) are

$$\Pr = \frac{\mu_{nl}}{\alpha_{bl}\rho_{nl}}, \quad Le = \frac{\alpha_{bl}}{D_B}, Lb = \frac{\alpha_{bl}}{D_m}, \quad Rb = \frac{h^3\Delta\rho_m g c}{D_m\mu_{nl}}, \quad Q = \frac{\sigma_{nl}(\mu_m)^2_{nl}H_0^2 h^2}{\mu_{nl}}, \quad Ra = \frac{g\beta_{nl}h^3(T_1^* - T_0^*)\rho_{nl}}{\mu_{nl}\alpha_{bl}}), \quad Ta = \frac{4\Omega^2 h^4}{\delta^2\mu_{nl}^2},$$
$$Rn = \frac{g\rho_{nl}\beta_\phi(\phi_1^* - \phi_0^*)h^3}{\mu_{nl}\alpha_{bl}}, \quad N_A = \frac{D_T(T_1^* - T_0^*)}{D_B T_0^*(\phi_1^* - \phi_0^*)}, \quad Pe = \frac{W_c h}{D_m}, \quad N_B = \frac{(\rho c)_{np}(\phi_1^* - \phi_0^*)}{(\rho c)_{nl}}.$$

3. Basic Solution

We assume that at the basic state,

$$\mathbf{v} = 0, p = p_b(z), \rho = \rho_b(z), T = T_b(z), \phi = \phi_b(z), \ n_b = n_b(z) \tag{16}$$

Substituting Eq. (16), Eqs. (10)-(13) transforms to

$$-\frac{dp_b}{dz} - Rm + RaT_b - Rn\phi_b - \frac{Rb}{Lbc}n_b = 0 \tag{17}$$

$$\frac{d^2T_b}{dz^2} + \frac{N_B}{Le}\frac{dT_b}{dz}.\frac{d\phi_b}{dz} + \frac{N_A N_B}{Le}\left(\frac{dT_b}{dz}\right)^2 = 0 \tag{18}$$

$$\frac{d^2\phi_b}{dz^2} + N_A\frac{d^2T_b}{dz^2} = 0 \tag{19}$$

$$n_b Pe - \frac{dn_b}{dz} = 0 \tag{20}$$

Integrating Eqs.(19) and using boundary conditions (14),(15) and we get

$$\phi_b = -N_A T_b + (1 - N_A)z + N_A \tag{21}$$

Substituting ϕ_b in Eq. (18), we get

$$\frac{d^2T_b}{dz^2}+\frac{(1-N_A)N_B}{Le}.\frac{dT_b}{dz}=0 \tag{22}$$

Solving this, we get

$$T_b=\left[\frac{1-\exp\left(-\frac{N_B(1-N_A)}{Le}(1-z)\right)}{1-\exp\left(-\frac{N_B}{Le}(1-N_A)\right)}\right]$$

As described by Buongiorno [38] and Nield and Kuznetsov [39], for most of the nanofluids, Le is of order 10^2 to 10^3, N_B is of order 10^{-2} to 10^{-5} and N_A is of order 10^0 to 10^1. Thus, exponents in T_b are neglected , so, it can be simplified as Nield and Kuznetsov [39], to obtain

$$T_b(z)=1-z \tag{23}$$

Putting T_b in Eq. (21) we get,

$$\phi_b(z)=z \tag{24}$$

Again, integrating Eq. (20), we get

$$n_b(z)=c\exp(Pe.z) \tag{25}$$

where c is the constant of integration given by

$$c=\frac{\bar{c}.Pe}{\exp(Pe)-1} \quad \text{and} \quad \bar{c}=\int_0^1 n_b(z)dz\ , \tag{26}$$

4. Perturbation

Perturbations are superimposed at the basic state as

$$\mathbf{v}=\varepsilon\mathbf{v}'(t,x,y,z),T=T_b(z)+\varepsilon T'(t,x,y,z),\phi=\phi_b(z)+\varepsilon\phi'(t,x,y,z),n=n_b(z)+\varepsilon n'(t,x,y,z),p=p_b(z)+\varepsilon p'(t,x,y,z),\hat{\mathbf{p}}=\hat{\mathbf{k}}+\varepsilon\mathbf{p}'(t,x,y,z) \tag{27}$$

Eqs. (10)-(13) transform to linear form

$$\nabla.\mathbf{v}'=0 \tag{28}$$

$$\frac{1}{\Pr}\frac{\partial\mathbf{v}'}{\partial t}+Q\mathbf{v}'-\sqrt{Ta}\left(\mathbf{v}'\times\hat{k}\right)+\nabla p'=\nabla^2\mathbf{v}'+\left(RaT'-Rn\phi'-\frac{Rb}{Lbc}n'\right)\hat{k} \tag{29}$$

$$\frac{\partial T'}{\partial t}-w'=\nabla^2T'+\frac{N_B}{Le}\left(\frac{\partial T'}{\partial z}-\frac{\partial\phi'}{\partial z}\right)-\frac{2N_AN_B}{Le}\frac{\partial T'}{\partial z} \tag{30}$$

$$\frac{\partial\phi'}{\partial t}+w'=\frac{1}{Le}\nabla^2\phi'+\frac{N_A}{Le}\nabla^2T' \tag{31}$$

$$\frac{\partial n'}{\partial t}=-\nabla.\left[n_b\left(\mathbf{v}'+\frac{Pe}{Lb}\hat{p}'\right)+n'\frac{Pe}{Lb}\hat{k}-\frac{1}{Lb}\nabla n'\right] \tag{32}$$

$$T'=0,\phi'=0,n'Pe=\frac{dn'}{dz}\ \text{ at } z=0 \text{ and } z=1 \tag{33}$$

The swimming direction of gyrotactic micro-organism is given by the following equation:

$$\hat{\mathbf{p}}'=GLb\left(\eta\hat{i}-\xi\hat{j}\right) \tag{34}$$

where $G=B.D_m/h^2$ is the Gyrotaxis number ([10];[11]),

$$\eta=-(1-\beta_0)\frac{\partial w'}{\partial x}+(1+\beta_0)\frac{\partial u'}{\partial z}\ ,\ \xi=(1-\beta_0)\frac{\partial w'}{\partial y}-(1+\beta_0)\frac{\partial v'}{\partial z},\ \beta_0=\frac{a_1^{\ 2}-b_1^{\ 2}}{a_1^{\ 2}+b_1^{\ 2}}\ , \tag{35}$$

where a_1, b_1, $B = a_{\perp}\mu_{nl} / 2l\rho_{nl}g$ and l can be found in ref. [10,11]. Using Eqs. (34), (35) in Eq. (32), we obtain

$$\frac{\partial n'}{\partial t} = -w'\frac{\partial n_b}{\partial z} - \frac{Pe}{Lb}\frac{\partial n'}{\partial z} + G.Pe.n_b\left[(1-\beta_0)\left(\frac{\partial^2 w'}{\partial x^2} + \frac{\partial^2 w'}{\partial y^2}\right) + (1+\beta_0)\frac{\partial^2 w'}{\partial z^2}\right] + \frac{1}{Lb}\nabla^2 n' \tag{36}$$

Taking curl in Eq. (29) for removing pressure term

$$\left(\frac{1}{\Pr}\frac{\partial}{\partial t} + Q - \nabla^2\right)\xi' - \sqrt{Ta}\frac{\partial \mathbf{v}'}{\partial z} - \left(RaT' - Rn\phi' - \frac{Rb}{Lbc}n'\right)\left(\nabla \times \hat{\mathbf{k}}\right) = 0 \tag{37}$$

where $\xi' = \nabla \times \mathbf{v}' = \xi_x\hat{\mathbf{i}} + \xi_y\hat{\mathbf{j}} + \xi_z\hat{\mathbf{k}}$ is the vorticity vector. Again, taking the curl of Eq. (37) using the identity $curl\,curl \equiv grad\,div - \nabla^2$ together with Eq. (28), we have

$$\left(\frac{1}{\Pr}\frac{\partial}{\partial t} + Q - \nabla^2\right)\nabla^2\mathbf{v}' + \sqrt{Ta}\frac{\partial \xi'}{\partial z} - \left(Ra\nabla_1{}^2T' - Rn\nabla_1{}^2\phi' - \frac{Rb}{Lbc}\nabla_1{}^2 n'\right)\hat{\mathbf{k}} = 0 \tag{38}$$

Now, taking a vertical component of Eqs. (37) and (38), we have

$$\left(\frac{1}{\Pr}\frac{\partial}{\partial t} + Q - \nabla^2\right)\xi_z{}' - \sqrt{Ta}\frac{\partial w'}{\partial z} = 0 \tag{39}$$

$$\left(\frac{1}{\Pr}\frac{\partial}{\partial t} + Q - \nabla^2\right)\nabla^2 w' + \sqrt{Ta}\frac{\partial \xi_z{}'}{\partial z} - \left(Ra\nabla_1{}^2T' - Rn\nabla_1{}^2\phi' - \frac{Rb}{Lbc}\nabla_1{}^2 n'\right) = 0 \tag{40}$$

We consider a stream function such that $u' = -\partial\psi'/\partial z$, $w' = \partial\psi'/\partial x$. On substituting this stream function, Eqs. (30), (31), (36), (39) and (40) transforms to

$$\left(\frac{1}{\Pr}\frac{\partial}{\partial t} + Q - \nabla^2\right)\xi_z{}' - \sqrt{Ta}\frac{\partial}{\partial z}\left(\frac{\partial\psi'}{\partial x}\right) = 0 \tag{41}$$

$$\left(\frac{1}{\Pr}\frac{\partial}{\partial t} + Q - \nabla^2\right)\nabla^2\left(\frac{\partial\psi'}{\partial x}\right) + \sqrt{Ta}\frac{\partial \xi_z{}'}{\partial z} - \left(Ra\nabla_1{}^2T' - Rn\nabla_1{}^2\phi' - \frac{Rb}{Lbc}\nabla_1{}^2 n'\right) = 0 \tag{42}$$

$$\frac{\partial T'}{\partial t} - \left(\frac{\partial\psi'}{\partial x}\right) = \nabla^2 T' + \frac{N_B}{Le}\left(\frac{\partial T'}{\partial z} - \frac{\partial\phi'}{\partial z}\right) - \frac{2N_A N_B}{Le}\frac{\partial T'}{\partial z} \tag{43}$$

$$\frac{\partial\phi'}{\partial t} + \frac{\partial\psi'}{\partial x} = \frac{1}{Le}\nabla^2\phi' + \frac{N_A}{Le}\nabla^2 T' \tag{44}$$

$$\frac{\partial n'}{\partial t} = -w'\frac{\partial n_b}{\partial z} - \frac{Pe}{Lb}\frac{\partial n'}{\partial z} + GPe.n_b\left[(1-\beta_0)\left(\frac{\partial^2}{\partial x^2}\left(\frac{\partial\psi'}{\partial x}\right) + \frac{\partial^2}{\partial y^2}\left(\frac{\partial\psi}{\partial x}\right)\right) + (1+\beta_0)\frac{\partial^2}{\partial z^2}\left(\frac{\partial\psi'}{\partial x}\right)\right] + \frac{1}{Lb}\nabla^2 n' \tag{45}$$

We take the perturbation quantities in the form as given by [40],

$$\psi' = \psi(z)\cos\beta x,\ \xi_z{}' = Z(z)\sin\beta x,\ T' = \Theta(z)\sin\beta x,\ \phi' = \Phi(z)\sin\beta x,\ n' = N(z)\sin\beta x \tag{46}$$

By substituting Eq.(46) into Eqs.(41)-(45),the linearized equations in dimensionless form reduces to

$$\left[Q - \left(D^2 - \beta^2\right)\right].Z + \beta\sqrt{Ta}D\psi = 0 \tag{47}$$

$$\beta\left[Q - \left(D^2 - \beta^2\right)\right].\left(D^2 - \beta^2\right)\psi - \sqrt{Ta}DZ - \beta^2.\left(Ra\Theta - Rn\Phi - \frac{Rb}{Lbc}N\right) = 0 \tag{48}$$

$$\beta\psi - \left(D^2 - \beta^2 + \frac{N_B}{Le}D - \frac{2N_A N_B}{Le}D\right)\Theta + \frac{N_B}{Le}D\Phi = 0 \tag{49}$$

$$\beta\psi + \frac{N_A}{Le}\left(D^2 - \beta^2\right)\Theta + \frac{1}{Le}\left(D^2 - \beta^2\right)\Phi = 0 \tag{50}$$

$$\beta cPe.e^{Pe.z}\left[1 + G\beta^2(1-\beta_0) - G(1+\beta_0)D^2\right]\psi + \left[\frac{1}{Lb}\left(D^2 - \beta^2\right) - \frac{Pe}{Lb}D\right]N = 0 \tag{51}$$

with boundary conditions

$$\Theta = \Phi = Z = 0, PeN = DN, z = 0 \text{ and } z = 1 \tag{52}$$

Here $D = d/dz$, β is dimensionless horizontal wave number such that $\beta = \sqrt{\beta_1^2 + \beta_2^2}$. The system of Eqs. (47)-(51) are solved for two sets of boundary conditions

(i) Both rigid boundaries

$$\psi = Z = D\psi = \Theta = \Phi = 0, PeN = DN, \qquad z = 0,1 \tag{53}$$

(ii)Lower rigid and upper free boundaries

$$\begin{aligned} &\psi = Z = D\psi = \Theta = \Phi = 0, PeN = DN, \quad z = 0 \\ &\psi = DZ = D^2\psi = \Theta = \Phi = 0, PeN = DN, \quad z = 1 \end{aligned} \tag{54}$$

5. Method of Solution

The higher order Galerkin method with number of terms N > 6, is employed with trial functions of waveform satisfying these boundary conditions:
(i) Both rigid boundaries:

$$\psi_i = \left(z^{(i+1)} - 2z^{(i+2)} + z^{(i+3)}\right), Z_i = \Theta_i = \Phi_i = \left(z^i - z^{(i+1)}\right), N_i = \left[2 - Pe\left(1 - 2z^i\right) - Pe^2\left(z^i - z^{(i+1)}\right)\right] \tag{55}$$

(ii) Lower rigid and upper free boundaries:

$$\begin{aligned} &\psi_i = z^2(1-z)\left(i + 2 - 2z^i\right), Z_i = \left[z^i.\left(z - \frac{1+i}{i}\right)\right], \Theta_i = \Phi_i = \left(z^i - z^{(i+1)}\right), N_i = \left[2 - Pe\left(1 - 2z^i\right) - Pe^2\left(z^i - z^{(i+1)}\right)\right], \\ &W_i, Z_i, \Theta_i, \Phi_i, N_i, i = 1,2,3,....M, \end{aligned} \tag{56}$$

such that,

$$\psi = \sum_{i=1}^{M} A_i.\psi_i, \quad Z = \sum_{i=1}^{M} B_i.Z_i, \quad \Theta = \sum_{i=1}^{M} C_i.\Theta_i, \quad \Phi = \sum_{i=1}^{M} D_i.\Phi_i, \quad N = \sum_{i=1}^{M} E_i.N_i \tag{57}$$

Substituting the trail functions (57) in the system of Eqs. (47)-(51) and after vanishing of the derived determinant of the coefficients, the analytical expression for stationary Rayleigh number Ra_{st} is evaluated in terms of other parameters.

5.1 Analytical Solution for Rigid Rigid boundaries

The non-trivial solution of the above homogeneous Eqs. (47)-(51) gives the expression for stationary Rayleigh number Ra for RR and RF boundary conditions.
(i) Ra stationary for rigid-rigid boundary conditions is

$$Ra_{st} = \frac{1}{F_4\beta^2}\left[19600F_5\left(F_2F_8\left(G\beta^2(\beta_0 - 1) - 1\right) + F_4F_7 - F_3F_8\right) - 313600F_1F_5F_8Gc - F_4Rn\beta^2(Le + N_A)\right] \tag{58}$$

where

$$F_1 = (1+\beta_0).\left(1 - e^{Pe}\right).\left(\frac{12}{Pe^2} + 1\right), F_2 = \frac{4c}{Pe}\left[\frac{\left(e^{Pe} - 1\right)}{Pe}.\left(13 + \frac{132}{Pe^2}\right) - \left(1 + e^{Pe}\right).\left(1 + \frac{66}{Pe^2}\right)\right], F_3 = \frac{96cG(1+\beta_0).\left(1 + e^{Pe}\right)}{Pe},$$

$$F_4 = \frac{4\beta^2}{Lb} - \frac{\beta^2 Pe^2}{3Lb} + \frac{Pe^4}{3Lb} + \frac{Pe^4\beta^2}{30Lb}, F_5 = \frac{\beta^2}{30} + \frac{1}{3}, F_6 = \frac{\beta^2}{30} + \frac{Q}{30} + \frac{1}{3}, F_7 = \frac{\beta^4}{630} + \frac{4\beta^2}{105} + \frac{2Q}{105} + \frac{Q\beta^2}{630} + \frac{4}{5} \; F_8 = -\frac{Rb\beta^2 Pe^2}{140Lbc} + \frac{Rb\beta^2}{15Lbc}$$

(ii) In the absence of magnetic field and rotation $(Q = Ta = 0)$, the stationary Rayleigh number Ra_{st} given by Eq. (58) reduces to

$$Ra_{st} = \frac{1}{F_4\beta^2}\left[19600F_5\left(F_2F_7\left(G\beta^2(\beta_0 - 1) - 1\right) + F_4F_6 - F_3F_7\right) - 313600F_1F_5F_7Gc - F_4Rn\beta^2(Le + N_A)\right] \tag{59}$$

where

$$F_1 = (1+\beta_0).\left(1 - e^{Pe}\right).\left(\frac{12}{Pe^2} + 1\right), F_2 = \frac{4c}{Pe}\left[\frac{\left(e^{Pe} - 1\right)}{Pe}.\left(13 + \frac{132}{Pe^2}\right) - \left(1 + e^{Pe}\right).\left(1 + \frac{66}{Pe^2}\right)\right], F_3 = \frac{96cG(1+\beta_0).\left(1 + e^{Pe}\right)}{Pe},$$

$$F_4 = \frac{4\beta^2}{Lb} - \frac{\beta^2 Pe^2}{3Lb} + \frac{Pe^4}{3Lb} + \frac{Pe^4\beta^2}{30Lb}, F_5 = \frac{\beta^2}{30} + \frac{1}{3}, F_6 = \frac{\beta^4}{630} + \frac{4\beta^2}{105} + \frac{4}{5}, F_7 = -\frac{Rb\beta^2 Pe^2}{140Lbc} + \frac{Rb\beta^2}{15Lbc}$$

this coincides with Eq. (51) in Kuznetsov [23].
(iii) In the non-appearance of rotation, magnetic field and micro-organisms, $Ta = Q = Rb = 0$, Ra stationary reduces to

$$Ra_{st} = \frac{1}{27\beta^2}\left[28\beta^6 - 27Rn\beta^2(Le + N_A) + 952\beta^4 + 20832\beta^2 + 141120\right] \tag{60}$$

which is identical with Eq. (77) in Nield and Kuznetsov [39] as well as Eq. (82) in Nield and Kuznetsov [41].

5.2 Analytical Solution for Rigid-Free boundaries

(i) Ra stationary for rigid-free boundary conditions is

$$Ra_{st} = \frac{1}{169F_6F_4\beta^2N_A}\begin{bmatrix}176400F_5F_6N_A.\left[F_1F_8G\beta^2(\beta_0-1)-F_2F_8(\beta_0+1)+F_8\left(F_3(\beta_0-1)-F_1\right)+F_4F_7\right]\\-169F_4F_6Rn\beta^2(Le+N_A)+3136F_4F_5TaN_A\end{bmatrix} \tag{61}$$

where

$$F_1 = c\left(\frac{1056\left(e^{Pe}-1\right)}{Pe^4}-\frac{444e^{Pe}}{Pe^3}+\frac{4e^{Pe}}{Pe}+\frac{54e^{Pe}}{Pe^2}-e^{Pe}-\frac{138}{Pe^2}-\frac{612}{Pe^3}-\frac{12}{Pe}\right), F_2 = cG\left(\frac{384}{Pe^2}-18e^{Pe}+\frac{216}{Pe}+42+\frac{168e^{Pe}}{Pe}\right), F_3 = \frac{384cGe^{Pe}}{Pe^2},$$

$$F_4 = \frac{4\beta^2}{Lb}-\frac{\beta^2Pe^2}{3Lb}+\frac{Pe^4}{3Lb}+\frac{Pe^4\beta^2}{30Lb}, F_5 = \frac{\beta^2}{30}+\frac{1}{3}, F_6 = \frac{8\beta^2}{15}+\frac{8Q}{15}+\frac{4}{3}, F_7 = \frac{19\beta^4}{630}+\frac{24\beta^2}{35}+\frac{19Q\beta^2}{630}+\frac{12Q}{35}+\frac{36}{5},$$

$$F_8 = -\frac{13Rb\beta^2Pe^2}{420Lbc}+\frac{Rb\beta^2Pe}{60Lbc}+\frac{3Rb\beta^2}{10Lbc}$$

(iii) Ra stationary for rigid-free boundary conditions without magnetic field and rotation is

$$Ra_{st} = \frac{1}{169F_4\beta^2N_A}\left[176400F_5N_A.\left[F_1F_8G\beta^2(\beta_0-1)-F_2F_8(\beta_0+1)+F_8\left(F_3(\beta_0-1)-F_1\right)+F_4F_7\right]-169F_4Rn\beta^2(Le+N_A)\right] \tag{62}$$

where

$$F_1 = c\left[\frac{1056\left(e^{Pe}-1\right)}{Pe^4}-\frac{444e^{Pe}}{Pe^3}+\frac{4e^{Pe}}{Pe}+\frac{54e^{Pe}}{Pe^2}-e^{Pe}-\frac{138}{Pe^2}-\frac{612}{Pe^3}-\frac{12}{Pe}\right], F_2 = cG\left[\frac{384}{Pe^2}-18e^{Pe}+\frac{216}{Pe}+42+\frac{168e^{Pe}}{Pe}\right], F_3 = \frac{384cGe^{Pe}}{Pe^2},$$
$$F_4 = \frac{4\beta^2}{Lb}-\frac{\beta^2Pe^2}{3Lb}+\frac{Pe^4}{3Lb}+\frac{Pe^4\beta^2}{30Lb}, F_5 = \frac{\beta^2}{30}+\frac{1}{3}, F_6 = \frac{8\beta^2}{15}+\frac{4}{3}, F_7 = \frac{19\beta^4}{630}+\frac{24\beta^2}{35}+\frac{36}{5}, F_8 = -\frac{13Rb\beta^2Pe^2}{420Lbc}+\frac{Rb\beta^2Pe}{60Lbc}+\frac{3Rb\beta^2}{10Lbc} \tag{63}$$

(iv) when $Ta = Q = Rb = 0$, Ra stationary reduces to

$$Ra_{st} = \frac{1}{507\beta^2}\left[532\beta^6-507Rn\beta^2(Le+N_A)+17416\beta^4+247968\beta^2+1270080\right] \tag{64}$$

which matches with Eq.(83) in Nield and Kuznetsov [39] and Eq.(16) in Yadav et al. [42].

5.3 Numerical Solution

In above section, the exact analytical solution for non-oscillatory convection is attained using one-term Galerkin method in Maple software for rigid-rigid and rigid-free boundaries. In order to get a more accurate solution, we have also solved the resulting eigenvalue problem numerically by shooting method with normalizing conditions X(4)=1 at z=1, after converting it into given set of ODE equations as shown below.

$$\left[X'(1),X'(2),X'(3),X'(5),X'(7),X'(9),X'(11)\right] = \left[X(2),X(3),X(4),X(6),X(8),X(10),X(12)\right],$$

$$X'(4) = -\left[\left(\frac{s}{\Pr}+Q\right)+\beta^2\right]X(1)+\left[\left(\frac{s}{\Pr}+Q\right)+2\beta^2\right].X(3)+\sqrt{Ta}.X(6)+\beta^2\left[\mathrm{Ra}.X(7)-Rn.X(9)\right]-\frac{Rb}{Lb.c}.\beta^2X(11),$$

$$X'(6) = \left(\frac{s}{\Pr}+Q+\beta^2\right).X(5)-\sqrt{Ta}.X(2), X'(8) = -X(1)+\left(\beta^2+s\right)X(7)+\frac{N_B}{Le}.\left[(2N_A-1)X(8)+X(10)\right], \tag{65}$$

$$X'(10) = Le.X(1)+N_A\beta^2X(7)+\left(Le.s+\beta^2\right)X(9)-N_A.\left[-X(1)+\left(\beta^2+s\right)X(7)+\frac{N_B}{Le}.\left[(2N_A-1)X(8)+X(10)\right]\right],$$

$$X'(12) = Lb\ c\ Pe.e^{Pe.z}\left[\left(1+G\beta^2(1-\beta_0)\right)X(1)-G(1+\beta_0)X(3)\right]+\left(sLb+\beta^2\right).X(11)+Pe.X(12)$$

Rigid-Rigid boundaries

$$X(1) = X'(1) = X(5) = X(7) = X(9) = 0, Pe.X(11) = X'(11) \qquad \text{at } z = 0,1 \tag{66}$$

Rigid-Free boundaries

$$\begin{aligned} &X(1) = X'(1) = X(5) = X(7) = X(9) = 0, Pe.X(11) = X'(11) \qquad \text{at } z = 0\\ &X(1) = X'(2) = X'(5) = X(7) = X(9) = 0, Pe.X(11) = X'(11) \qquad \text{at } z = 1 \end{aligned} \tag{67}$$

where $X(1) = \psi(z)$, $X(5) = Z(z)$, $X(7) = \Theta(z)$, $X(9) = \Phi(z)$, $X(11) = N(z)$ are unknown functions to be determined and here the prime operator denotes the ordinary derivative w.r.t. z.

We have validated our results for RR and RF boundary conditions for different values of Taylor number Ta, in the absence of magnetic field Q, for the limiting case of nanofluid $(Rn = N_A = N_B = 0)$ in Table 1 and 2. We have correlated critical Rayleigh number Ra_c and corresponding wave number β_c with the results of Yadav et al. [43] and Chandrasekhar [44]. Also, some of the numerical results are presented in Table 3 and Table 4 for RR and RF boundaries for different values of controlling parameters.

Table 1. Numerical validation of Ra_c and β_c for different values of Ta for RR case in the absence of magnetic field $(Q = 0)$ for regular fluids.

Ta	Chandrasekhar [44]		Yadav et.al. [43]		Present Result	
	β_c	Ra_c	β_c	Ra_c	β_c	Ra_c
0	3.13	1707.8	3.12	1707.83	3.12	1707.76
10	3.10	1713.0	3.12	1712.74	3.12	1712.67
100	3.15	1756.60	3.16	1756.41	3.16	1756.35
500	3.30	1940.30	3.32	1940.26	3.32	1940.20
1000	3.50	2151.70	3.49	2151.39	3.49	2151.34
2000	3.75	2530.50	3.75	2530.18	3.75	2530.13
5000	4.25	3469.20	4.27	3468.58	4.28	3468.49
7500	-	-	-	-	4.56	4124.24
10000	4.80	4713.10	4.79	4712.13	4.79	4712.04
20000	-	-	-	-	5.40	6684.26

Table 2. Numerical validation of Ra_c and β_c for different values of Ta for RF case in the absence of magnetic field $(Q = 0)$ for regular fluids.

Ta	Chandrasekhar [44]		Yadav et al. [43]		Present result	
	β_c	Ra_c	β_c	Ra_c	β_c	Ra_c
0	2.68	1100.75	2.68	1100.77	2.68	1100.65
6.25	2.68	1108.50	2.70	1107.85	2.70	1107.73
31.25	2.70	1135.90	2.74	1135.53	2.74	1135.41
62.50	2.79	1169.50	2.80	1168.84	2.80	1168.72
187.5	2.96	1291.70	2.98	1290.90	2.98	1290.80
625.0	3.40	1637.60	3.39	1637.44	3.39	1637.40
1875.0	4.00	2360.30	4.01	2358.27	4.01	2358.33
2000.0	-	-	-	-	4.05	2419.48

Table 3. Critical Rayleigh number Ra_c and critical wave number β_c for RR and RF boundaries (default set)

Ta	Rigid- Rigid		Rigid-Free		Rigid-Rigid		Rigid-Free		Rigid-Rigid		Rigid-Free	
	β_c	Ra_c	β_c	Ra_c	β_c	Ra_c	β_c	Ra_c	β_c	Ra_c	β_c	Ra_c
	$Rn = 90$				$Rn = 100$				$Rn = 110$			
0	3.2310	13387.1519	3.1420	12086.1163	3.2310	12367.1513	3.1420	11066.1140	3.2310	11347.1494	3.1420	10046.1221
10	3.2310	13387.5167	3.1420	12086.4962	3.2310	12367.5160	3.1420	11066.4939	3.2310	11347.5142	3.1420	10046.5019
100	3.2310	13390.7994	3.1422	12089.9149	3.2310	12370.7987	3.1422	11069.9126	3.2310	11350.7969	3.1422	10049.9206
500	3.2320	13405.3868	3.1434	12105.1050	3.2320	12385.3862	3.1434	11085.1027	3.2320	11365.3843	3.1434	10065.1108
1000	3.2331	13423.6123	3.1450	12124.0836	3.2331	12403.6116	3.1450	11104.0812	3.2331	11383.6098	3.1450	10084.0893
5000	3.2433	13569.0696	3.1560	12275.5438	3.2433	12549.0690	3.1560	11255.5416	3.2433	11529.0712	3.1560	10235.5497
10000	3.2560	13750.0372	3.1700	12463.9683	3.2560	12730.0366	3.1700	11443.9661	3.2560	11710.0428	3.1700	10423.9743
Rb	$Pe = 4$				$Pe = 4.1$				$Pe = 4.2$			
0	3.2320	12541.4669	3.1584	11404.4630	3.2320	12541.4669	3.1584	11404.4877	3.2320	12541.4669	3.1584	11404.4630
5	3.2340	12311.5881	3.1352	10899.1356	3.2350	12298.6439	3.1330	10852.3403	3.2355	12285.4452	3.1310	10801.1774
10	3.2360	12081.1059	3.1092	10369.0404	3.2372	12055.1264	3.1041	10269.1146	3.2391	12028.6269	3.0984	10158.8388
20	3.2400	11618.3053	3.0471	9221.5302	3.2430	11565.9767	3.1000	9000.0195	3.2470	11512.5557	3.0175	8729.9333
30	3.2440	11153.0111	2.9670	7929.1825	3.2490	11073.9467	3.1000	7572.5368	3.2550	10993.1574	2.9042	7044.4382
50	3.2530	10214.7176	2.7130	4687.4679	3.2620	10080.9418	3.1000	4051.8506	3.2722	9943.9679	2.4580	2277.3006
Q	$N_A = 2$				$N_A = 3$				$N_A = 5$			
500	3.2331	12403.6117	3.1450	11104.0813	3.2331	12303.6114	3.1450	11004.0912	3.2331	12103.6111	3.1450	10804.0802
1000	3.2160	32829.2177	3.1563	31190.3715	3.2160	32729.2172	3.1563	31090.4927	3.2160	32529.2164	3.1563	30890.3696
2000	3.1990	73313.2686	3.1590	71175.3616	3.1990	73213.2677	3.1590	71075.7662	3.1990	73013.2662	3.1590	70875.3583
3000	3.1904	113574.0597	3.1584	111046.6156	3.1904	113474.3047	3.1584	110947.4658	3.1904	113274.3023	3.1584	110746.6111
5000	3.1810	193781.3645	3.1570	190629.1593	3.1810	193681.3624	3.1570	190534.7116	3.1810	193481.3584	3.1570	190329.1522
7500	3.1745	293730.2670	3.1550	289950.6070	3.1745	293630.2639	3.1550	289860.2603	3.1745	293430.2579	3.1550	289650.5970

Table 4. Critical Bio-convection Rayleigh number Rb_c and critical wave number β_c for RR and RF boundaries.

Ta	Rigid-Rigid		Rigid-Free		Rigid-Rigid		Rigid-Free		Rigid-Rigid		Rigid-Free	
	β_c	Rb_c	β_c	Rb_c	β_c	Rb_c	β_c	Rb_c	β_c	Rb_c	β_c	Rb_c
	$Le = 100$				$Le = 110$				$Le = 120$			
0	3.2520	53.7811	3.0891	12.9893	3.2420	32.50029	3.1390	3.6487	3.2334	10.9680	2.6680	0.0086
10	3.2520	53.8576	3.0892	13.0241	3.2423	32.57797	3.1390	3.6859	3.2335	10.9759	2.6680	0.0045
100	3.2550	54.5454	3.0901	13.3366	3.2450	33.27643	3.1400	4.0203	3.2340	11.0469	2.6693	0.0010
500	3.2580	55.3083	3.0911	13.6829	3.2480	34.05118	3.1410	4.3909	3.2350	11.3623	2.6760	0.0070
1000	3.2673	57.5889	3.0941	14.7167	3.2570	36.36724	3.1441	5.4962	3.2363	11.7562	2.6840	0.0026
5000	3.2830	61.3632	3.0990	16.4223	3.2720	40.20031	3.1493	7.3177	3.2480	14.8950	2.7544	0.0005
10000	3.3141	68.8141	3.1090	19.7716	3.3020	47.7675	3.1600	10.8874	3.2623	18.7877	2.8620	0.0065
Ra	$Rn = 90$				$Rn = 100$				$Rn = 110$			
500	3.5130	261.8848	2.0760	70.3429	3.4632	243.2215	2.2325	67.3191	3.4230	224.2127	2.3704	63.8513
1000	3.4871	252.7812	2.1552	68.9156	3.4424	233.9458	2.3022	65.6757	3.4060	214.7751	2.4323	61.9842
2000	3.4432	234.3193	2.2995	65.7438	3.4062	215.1551	2.4300	62.0614	3.3754	195.6721	2.5470	57.9046
5000	3.3510	177.0577	2.6460	53.5308	3.3282	156.9896	2.7410	48.3529	3.3090	136.6324	2.8271	42.5824
7500	3.3011	127.3602	2.8633	39.7726	3.2854	106.5947	2.9380	33.0456	3.2720	85.5542	3.0050	25.5867
10000	3.2662	75.9773	3.0330	21.9672	3.2550	54.5454	3.0901	13.3366	3.2450	32.8485	3.1410	3.8251

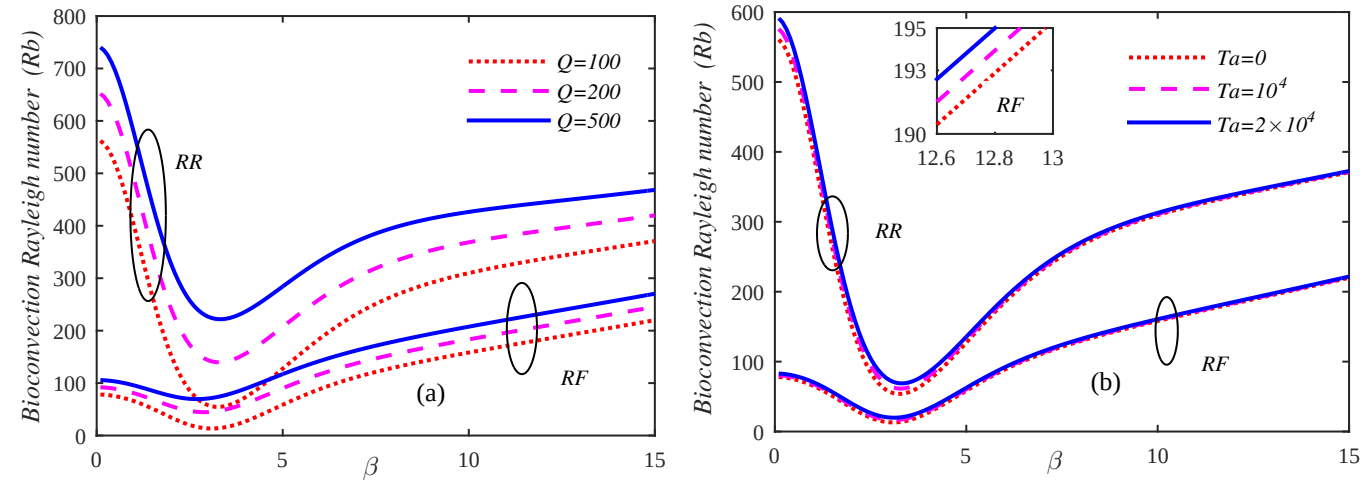

Fig. 2. Effect of (a) Q and (b) *Ta* on Bio-Rayleigh number *Rb*

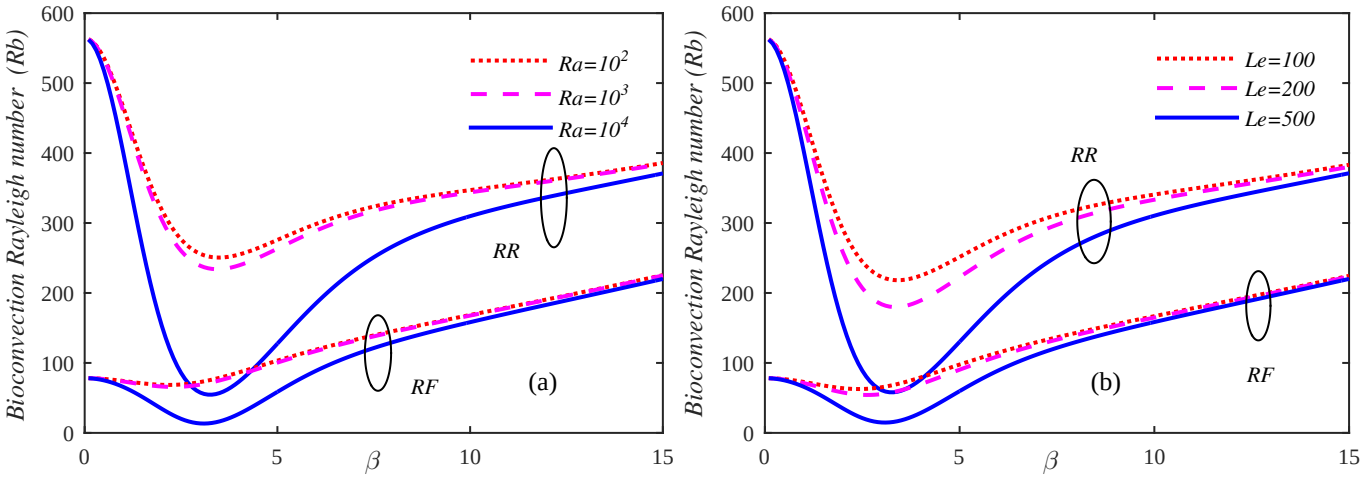

Fig. 3. Effect of (a) *Ra* and (b) *Le* on Bio-Rayleigh number *Rb*

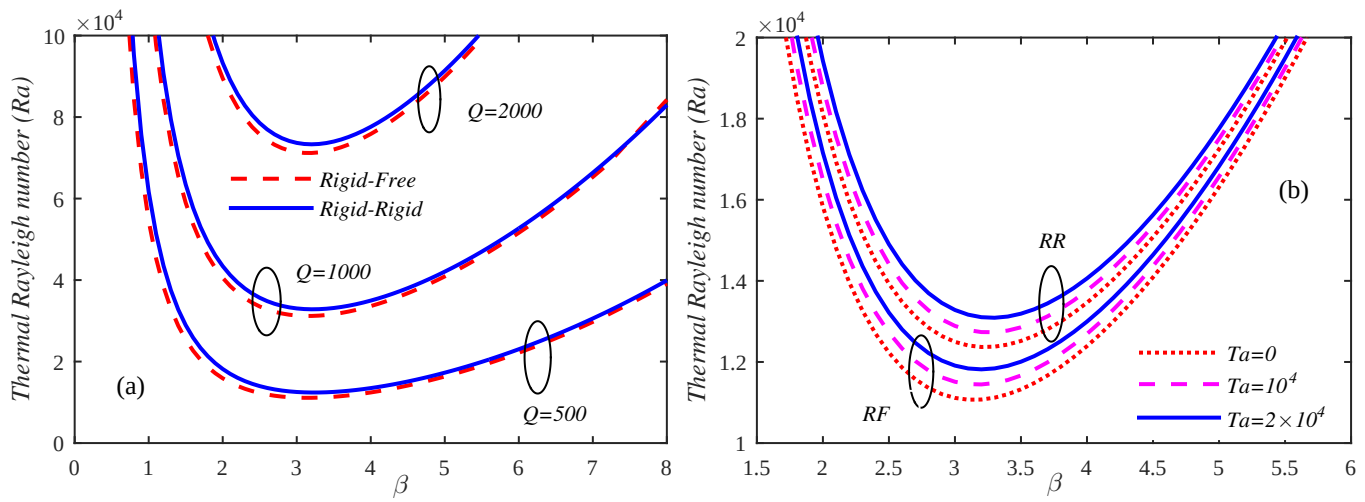

Fig. 4. Effect of (a) Q and (b) *Ta* on Thermal-Rayleigh number *Ra*

6. Results and Discussion

The stability analysis of bioconvection in the fluid layer containing nanoparticles and gyrotactic microorganisms in addition to magnetic field and rotation is carried out. According to Buongiorno [38], the data for alumina/water nanofluid is taken as follows:

$$\phi_1^* - \phi_0^* = 0.001 \text{ , } \phi_0^* = 0.01 \;\; \rho_{nl} = 1000 Kg/m^3 \text{ , } \mu_{nl} = 10^{-3} Pa \text{ , } \rho_{np} = 4\times 10^3 Kg/m^3 \text{ , } \alpha_{nl} = 2\times 10^{-7} m^2/s \text{ , } D_T = 6\times 10^{-11} m^2/s$$
$$(\rho c)_{np} = 3.1\times 10^6 J/m^3 \text{ , } (\rho c)_{bl} = 4\times 10^6 J/m^3 \text{ , } \beta_{nl} = 3.4\times 10^{-3} 1/K \text{ , } T_1^* = 300K \text{ , } T_0^* - T_1^* = 1K \text{ , } D_B = 4\times 10^{-11} m^2/s \text{ .}$$

Also, the parametric values used for alga Chlamydomonas nivalis presented by Pedley et al. [10], Hill et al. [12] are:

$$D_m = 5\times 10^{-8} m^2/s \text{ , } W_c = 10^{-4} m/s \text{ , } \beta_0 = 0.31 \text{ , } \;\; \Delta\rho_m = 50 Kg/m^3 \text{ , } \theta = 5\times 10^{-16} m^3 \text{ , } h = 2\times 10^{-3} mm$$

Based on these values, the following dimensionless parameters are estimated as:

$$\Pr = 5 \text{ , } Ra = 1.4\times 10^4 \text{ , } Rn = 1.2\times 10^3 \text{ , } Rb = 3 \text{ , } c = 3.7\times 10^{-5} \text{ , } N_A = 5 \text{ , } N_B = 7.5\times 10^{-4} \text{ , } Le = 5000 \text{ , } G = 0.03 \text{ , } Pe = 4 \text{ , } Lb = 4$$

The analytical expressions for stationary Rayleigh number are obtained using the one-term Galerkin technique which is presented in Eq. (58) and Eq. (61). Results have been plotted for alumina/water nanofluid using higher-order Galerkin method to get better accuracy.

In Figs. 2 and 3, neutral stability curves have been plotted on (β, Rb) plane for varying parameters Chandrasekhar number Q, Taylor number Ta, Thermal Rayleigh number Ra and Lewis number Le. Also in Fig. 4, wave number β as a function of thermal Rayleigh number Ra is plotted on (x, y) plane for rigid-rigid and rigid-free boundaries for different values of Q and Ta. The default set has been taken $Q = 500$, $Ta = 1000$, $Lb = 4$, $Pe = 4$, $N_A = 2$, $N_B = 0.01$, $Le = 100$, $Rb = 3$, $Rn = 100$. In Fig. 3(b), for plotting with Lewis number Le, $Rn = 20$ has been fixed just to maintain the minimum value of their product $(Le * Rn > 2000)$ so as to obtain positive Rayleigh number and $Rn = 100$ is taken as a default parameter, the results are depicted in the form of neutral curves separating the region in two zones: unstable (above) and stable (below) which further articulates the conduction/convection dominance. In Figs. 2(a) and 2(b), we observe that the effect of increasing Q and Ta is to increase the critical values of Bio-Rayleigh number Rb. Thus, convection due to up swimming of microorganisms is delayed by rotation and magnetic field by suppressing the vertical motion in the nanofluid layer. Also, magnetic field stabilizes the system faster than rotation.

In Figs. 3(a),(b), we notice that Rb decreases with increasing Ra and Le. It depicts that microorganisms move faster in lower and upper part of the nanofluid layer and convection due to these increases as heat and mass transfer increases. So, both thermal Rayleigh number and Lewis number destabilizes the system. Also, we observe that in all these figures, the most unstable wave number is between 2 to 4 for $Q = 100$, $Ta = 0$, $Ra = 10000$ and $Le = 500$ for rigid-free boundaries. The distinct values of Q and Ta taken in fig. 4(a), (b) are 500, 1000, 2000 and 0, 10000, 20000 respectively. In these plots, we examine that Ra increases with an increase in both magnetic field and rotation but this increment is very slow in rotation in comparison to magnetic field. Thus, the convection due to temperature variation is slowed down due to rotation and magnetic field which stabilizes the system. Also, in Fig. 4(a) and 4(b), the marginal stability curve approaches to Ra_c at 11108.6171 for $Q = 500$ and 11070.0925 for $Ta = 0$ respectively for $\beta_c = 3.1$.

Fig. 5, disports the impact of rotation parameter Ta, on the minimum value of thermal Rayleigh number, Ra_c and the corresponding wave number, β_c for Bio-Rayleigh number $Rb = 0, 10, 50$. These figures depict that Ra_c as well as β_c increases with increasing Ta. Also, we observe in Fig. 5(a) that Ra_c decreases with increasing Rb for both rigid-rigid and rigid-free boundaries, but in Fig. 5(b), β_c increases with increasing Rb for rigid-rigid boundaries while decreases with increasing Rb for rigid-free boundaries. It shows that convection goes on faster with the enhancement of microorganisms in the nanofluid layer.

Fig. 6 displays a relation between Rayleigh number Ra and critical Bio-Rayleigh number Rb_c, critical wave number β_c and Rayleigh number Ra for specific values of Q. In Fig. 6(a), we observe that for small values of Ra, Rb_c remains constant, but for large Ra, it goes on decreasing rapidly which implies that the increment in the temperature variation helps in the development of bioconvection across the suspension layer and destabilizes the system. Also Rb_c increases fastly for both rigid-rigid and rigid-free boundaries with increasing Q.

Also, we observe that minimum values of Rb_c for rigid-free and rigid-rigid boundaries for $Q = 500$ are 68.826 and 252.231 respectively while its maximum values for $Q = 1000$ are 146.345 and 627.548 respectively. In Fig. 6(b), we analyze that as Ra increases, β_c increases for rigid free boundaries while its behavior is reverse for rigid-rigid boundaries. Also for increasing Q, β_c decreases for rigid-free boundaries and increases for rigid-rigid boundaries. Moreover, in all figures, we analyze that rigid-rigid boundaries are more stable in comparison to rigid-free boundaries. Fig. 7 shows the variation in streamlines, iso-therms and iso-nanoconcentrations of the disturbance (ten times) shapes of $\psi(z)\cos ax$, $\Theta(z)\sin ax$, $\Phi(z)\sin ax$ for rigid-rigid (RR) and rigid-free (RF) boundaries at their critical state in (X, Z) space. The filled contours of disturbances are symmetrical at X=1 and adjoining opposite cells in all the cases and the concentration of temperature and nanoparticle fields has comparatively weak cells for Rigid-Free (RF) than Rigid-Rigid (RR). In other words, the flow patterns are independent of boundary conditions (RR or RF) but the slight variation in their magnitudes implying advances or delays the convection.

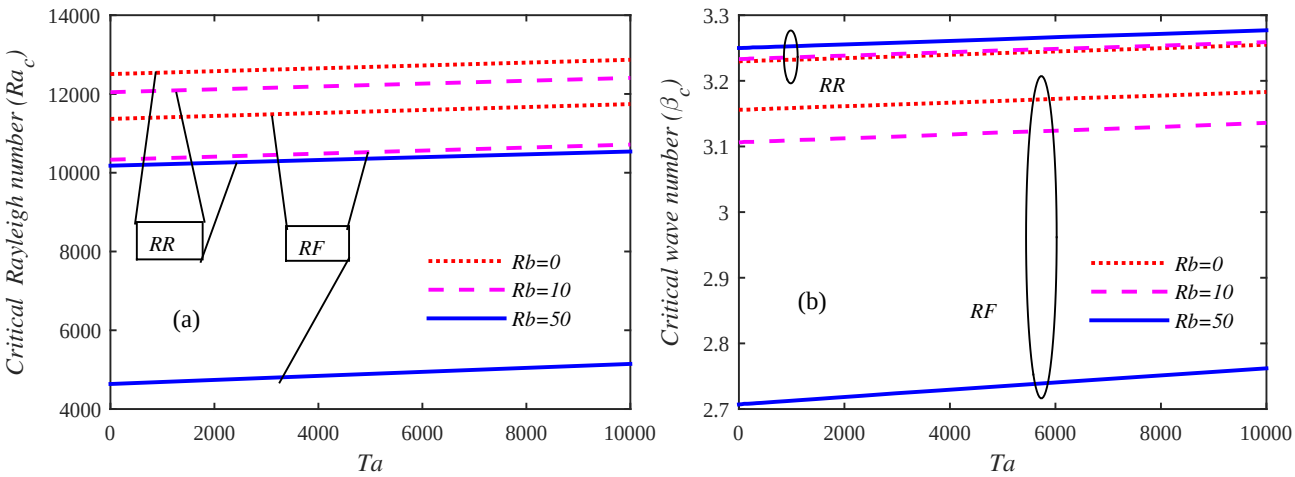

Fig. 5. Relation between (a) Ra_c and Ta (b) a_c and Ta for various Rb

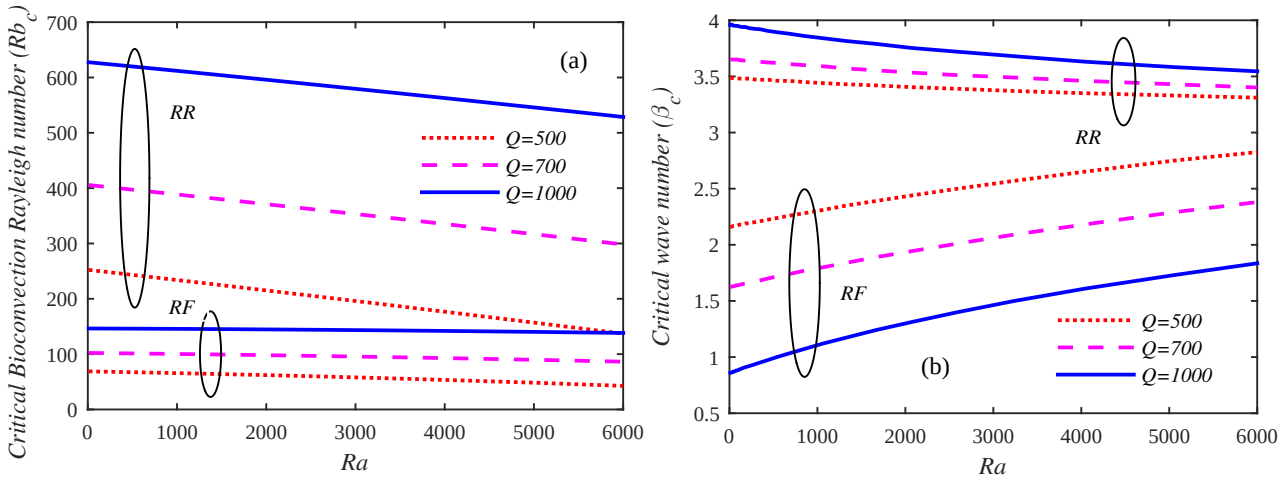

Fig. 6. Relation between (a) Ra_c and Ta (b) a_c and Ta for various Rb

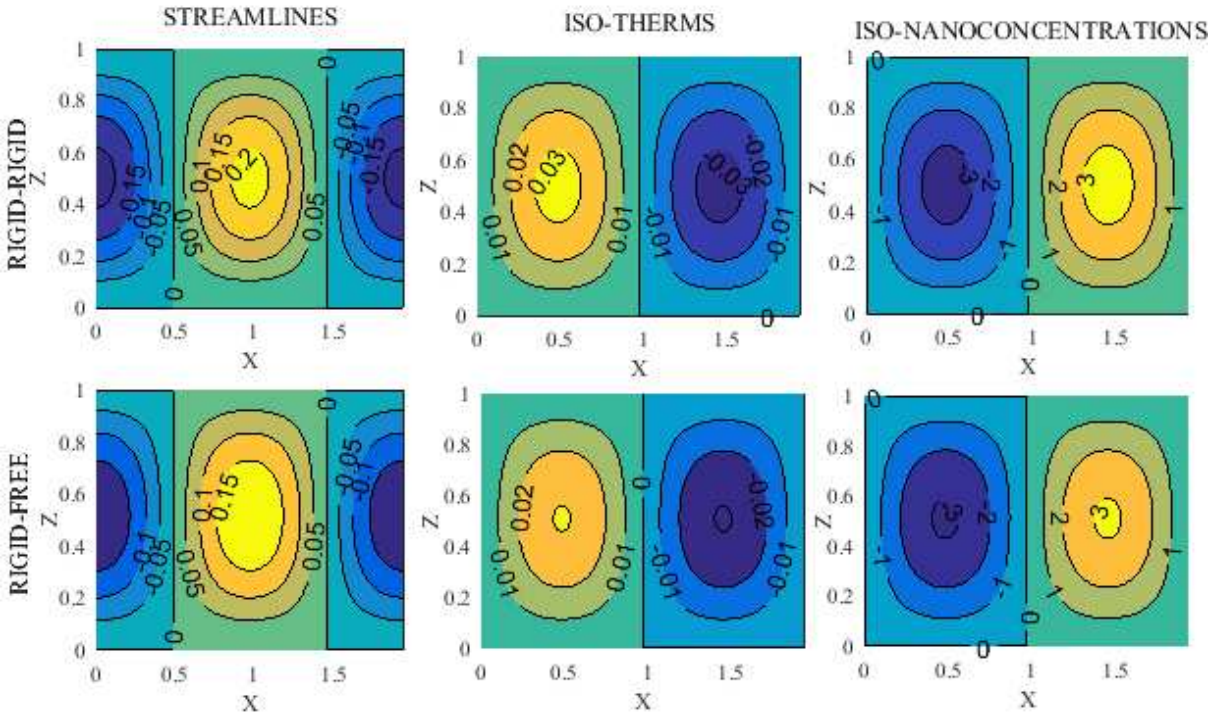

Fig. 7. Disturbances behavior for both Rigid-Rigid (RR) and Rigid-Free (RF) boundaries

7. Conclusion

In this paper, we have examined the effect of microorganisms in water-based nano-liquid on the onset of convection. Rotation and magnetic field play significant role on the stability analysis of bioconvection in the nanofluid layer. The governing system is solved both analytically and numerically for rigid-rigid and rigid-free boundary conditions. It is noted that both Chandrasekhar number and Taylor number increase thermal Rayleigh number as well as bioconvection Rayleigh number in the nanofluid layer. Thus, the convection is delayed down due to both magnetic field and rotation. Also we analyze that Rb_c decreases with increasing Ra and the trend is the same for thermal Rayleigh number with Rb. Thus, increasing temperature variation helps in the up swimming of microorganisms in the upper and lower part of the nanofluid layer and so destabilizes the system. Also, the dynamical system is found to be more stable when both boundaries are rigid while rigid-free boundaries are least stable.

Nomenclature

a_1	Semi-major axis of a spheroidal microorganism
b_1	Semi-minor axis of a spheroidal microorganism
c	Dimensionless parameter defined by Eq. (26)
$\bar{c}$	Dimensionless average concentration of microorganisms
D_B	Brownian diffusion coefficient [m^2/s]
D_m	Diffusivity of microorganisms [m^2/s]
D_T	Thermophoretic diffusion coefficient [m^2/s]
g	Gravity [m/s^2]
G	Gyrotaxis number
h	Height of nanofluid layer [m]
H_0	Magnetic field strength (A/m)
j^*	Flux of microorganisms [T]
k_{nl}	Nanofluid thermal conductivity [W.m^{-1}.K^{-1}]
Lb	Bioconvection Lewis number
Le	Lewis number for Brownian diffusion of nanoparticles
n^*	Concentration of microorganisms
n	Dimensionless concentration micro-organisms
N_A	Modified diffusivity ratio
N_B	Modified Particle density increment
p^*	Pressure [Pa]
p	Dimensionless pressure
$\hat{\mathbf{p}}$	Unit vector indicating the average direction of microorganisms swimming
Pe	Peclet number
Q	Chandrasekhar number
Ra	Thermal Rayleigh number
Rb	Bioconvection Rayleigh number
Rn	Concentration Rayleigh number
t^*	Time [s]
t	Dimensionless time
T^*	Nanofluid temperature [K]
T	Dimensionless Nanofluid temperature [K]
T_0^*	Upper wall temperature [K]
T_1^*	Lower wall temperature [K]
Ta	Taylor number
$W_c\hat{\mathbf{p}}$	Vector of the average microorganisms swimming velocity
(u,v,w)	Dimensionless velocity components [m/s]
$\mathbf{v}^*$	Nanofluid velocity, (u^*,v^*,w^*) [m/s]
(x^*,y^*,z^*)	Cartesian co-ordinates [m]
(x,y,z)	Dimensionless Cartesian co-ordinates

Greek Symbols

$\alpha_\perp$	Dimensionless constant (viscous torque to the angular velocity of the cell)
α_{bl}	Thermal diffusivity of base liquid [m^2/s]
α_{nl}	Thermal diffusivity of nano-liquid [m^2/s]
β	Horizontal wave number
β_0	Measure of the cell eccentricity
β_{nl}	Nanofluid thermal expansion coefficient [K^{-1}]
β_ϕ	Nanoparticles thermal expansion coefficient [K^{-1}]
δ	Amplitude of gravity modulation
$\Delta\rho_m$	Density difference between a cell and base fluid $(\rho_{cell}-\rho_{bl})$
$(\mu_m)_{nl}$	Magnetic permeability of nano-liquid [N.A^{-2}]
μ_{nl}	Dynamic viscosity of nano-liquid [kg.m.s^{-1}]
θ	Average volume of microorganisms [m^3]
Ω^*	Angular velocity in vertical direction(rad/s)
ρ_{nl}	Nanofluid density [kg/m^3]
ρ_{bl}	Density of base liquid [kg/m^3]
σ_{nl}	Electrical conductivity of nano-liquid [S/m]
$(\rho c)_{nl}$	Volumetric heat capacity of nano-liquid [J/K]
$(\rho c)_{np}$	Volumetric heat capacity of nanoparticles [J/K]
ϕ^*	Nanoparticle volume fraction
ϕ	Dimensionless nanoparticle volume fraction
ϕ_0^*	Lower wall nano-concentration
ϕ_1^*	Upper wall nano-concentration

Subscripts

b	Basic state
bl	Base-liquid
nl	Nano-liquid
np	Nanoparticles

Superscripts

*	Dimensional variable

Author Contributions

M. Khurana planned and initiated the project and suggested the appropriate mathematical model for present nanofluid bio-convection problem. P. Rana performed the linear stability analysis and developed the MATLAB and MAPLE codes. S. Srivastava

revised the manuscript and provided graphical software assistance. All authors discussed the results, reviewed and approved the final version of the manuscript.

Conflict of Interest

The authors declared no potential conflicts of interest with respect to the research, authorship and publication of this article.

Funding

The authors received no financial support for the research, authorship and publication of this article.

References

[1] Sokolov, A., Goldstein, R.E., Feldchtein, F.I., Aranson, I.S., Enhanced mixing and spatial instability in concentrated bacterial suspensions, *Physical Review* E, 80(3), 2009, 031903.
[2] Murshed, S.M.S., Castro, C.N.de., Heat Transfer of Nanofluids in Microsystems, *The 26th International Symposium on Transport Phenomena (ISTP-26)*, Leoben, Austria, 2015.
[3] Ebrahimi, S., Sabbaghzadeh, J., Maryamalsadat, L.,Iraj, H., Cooling performance of a microchannel heat sink with nanofluids containing cylindrical nanoparticles (carbon nanotubes), *Heat and Mass Transfer*, 46, 2010, 549-553.
[4] Sedarous S.S., Attlesey, C.D., Nanofluids for use in electronics, *Patent Application Publication*, US 2012/0186789A1.
[5] Fan, X., Chen, H., Ding, Y., Plucinski, P.K., Lapkin, A.A., Potential of 'nanofluids' to further intensify micro reactors, *Green Chemistry*, 10, 2008, 670-677.
[6] Do, K.H., Jang, S.P., Effect of nanofluids on the thermal performance of a flat micro heat pipe with a rectangular grooved wick, *Journal of Heat and Mass Transfer*, 53(9), 2010, 2183-2192.
[7] Wong, K.V., Leon, O.De., Applications of Nanofluids: Current and Future, *Advances in Mechanical Engineering*, 2, 2010, 519659.
[8] Li, H., Liu, S., Dai, Z., Bao, J., Yang, X., Applications of Nanofluids in Electrochemical Enzyme Biosensors, *Sensors (Besel)*, 9, 2009, 8547-8561.
[9] Plesset, M.S., Winet, H., Bioconvection patterns in swimming microorganism cultures as an example of Rayleigh-Taylor instability, *Nature*, 248, 1974, 441-443.
[10] Childress, S., Levandowsky, M., Spiegel, E.A., Pattern formation in a suspension of swimming microorganisms: equations and stability theory, *Journal of Fluid Mechanics,* 69(3), 1975, 591-613.
[11] Pedley, T.J., Hill, N.A., Kessler, J.O., The growth of bioconvection patterns in a uniform suspensions of gyrotactic micro-organisms, *Journal of Fluid Mechanics*, 195, 1988, 223-237.
[12] Pedley, T.J., Kessler, J.O., James, L.M., The orientation of spheroidal microorganisms swimming in a flow field, *Proceedings of the Royal Society of London. Series B. Biological Sciences*, 231, 1987, 47–70.
[13] Hill, N.A., Pedley, T.J., Kessler, J.O., Growth of bioconvection patterns in a suspension of gyrotactic microorganisms in a layer of finite depth, *Journal of Fluid Mechanics*, 208, 1989, 509-543.
[14] Nield, N.A., Kuznetsov, A.V., The onset of bio-thermal convection in a suspension of gyrotactic microorganisms in a fluid layer: Oscillatory convection, *International Journal of Thermal Sciences*, 45(10), 2006, 990-997.
[15] Zhao, M., Xiao, Y., Wang, S., Linear stability of thermal bioconvection in a suspension of gyrotactic micro-organisms, *International Journal of Heat and Mass Transfer,* 126(Part A), 2018, 95-102.
[16] Amirsom, N.A., Uddin, M.J., Basir, M.F.M, Kadir, A., Beg, O.A., Ismail, A.I.M., Computation of Melting Dissipative Magnetohydrodynamic Nanofluid Bioconvection with Second order Slip and Variable Thermophysical Properties, *Applied Sciences*, 9(12), 2019, 1-19.
[17] Basir, M.F.M., Hafidzuddin, M.E.H., Naganthran, K., Hashim, Kasihmuddin, M.S.M., Stability analysis of unsteady stagnation-point gyrotactic bioconvection flow and heat transfer towards the moving sheet in a nanofluid, *Chinese Journal of Physics*, 65, 2020, 538-553.
[18] Bala, C.S., Alluguvelli, R., Naikoiti, K., Makinde, O.D., Effect of Chemical Reaction on Bioconvective Flow in Oxytactic Microorganisms Suspended Porous Cavity, *Journal of Applied and Computational Mechanics*, 6(3), 2020, 653-664.
[19] Kuznetsov, A.V., Avramenko, A., Effect of small particles on the stability of bioconvection in a suspension of gyrotactic microorganisms in a layer of finite depth, *International Communications in Heat and Mass Transfer*, 31(1), 2004, 1-10.
[20] Kuznetsov, A.V., Geng, P., The interaction of bioconvection caused by gyrotactic micro-organisms and settling of solid particles, *International Journal of Numerical Methods for Heat & Fluid Flow*, 15(4), 2005, 328-347.
[21] Geng, P., Kuznetsov, A.V., Effect of small solid particles on the development of bioconvection plumes, *International Communications in Heat and Mass Transfer*, 31(5), 2004, 629-638.
[22] Kuznetsov, A.V., Avramenko, Stability Analysis of Bioconvection of Gyrotactic Motile Microorganisms in a Fluid Saturated Porous Medium, *Transport in Porous Media*, 53, 2003, 95-104.
[23] Kuznetsov, A.V., The onset of nanofluid bioconvection in a suspension containing both nanoparticles and gyrotactic microorganisms, *International Communications in Heat and Mass Transfer*, 37(10), 2010, 1421-1425.
[24] Kuznetsov, A.V., Non-oscillatory and oscillatory nanofluid bio-thermal convection in a horizontal layer of finite depth, *European Journal of Mechanics B/Fluids*, 30(2), 2011, 156-165.
[25] Xiong, X., Lidstrom, M.E., Parviz, B.A., Microorganisms for MEMS, *Journal of Microelectromechanical Systems,* 16(2), 2007, 429-444.
[26] Sonetha, V., Agarwal, P., Doshi, S., Kumar, R., Mehta, B., Microelectromechanical Systems in Medicine, *Journal of Medical and Biological Engineering*, 37, 2017, 580-601.
[27] Asif, A., Khawaldeh, S., Khan, M.S., Tekin, A., Design and Simulation of microfluidics device for metabolicscreening and quantitative monitoring of drug uptake in cancer cells, *Journal of Electrical Bioimpedance*, 9(1), 2018, 10-16.
[28] Ray, A.K.,B.V., Anwar Beg, O., Gorla, R.S.R., Murthy, P.V.S.N., Magneto-bioconvection flow of a casson thin filmwith nanoparticles over an unsteady stretching sheet: HAM and GDQ computation, *International Journal of Numerical Methods for Heat & Fluid Flow*, 29(11), 2019, 4277-4309.
[29] Khan, N.S., Kumam, P., Thounthong, P., Second law analysis with effects of Arrhenius activation energy and binary chemical reaction on nanofluid flow, *Scientific Reports*, 10, 2020, 1226.
[30] Khan, N.S., Shah, Z., Shutaywi, M., Kumam, P., Thounthong, P., A comprehensive study to the assessment of Arrhenius activation energy and binary chemical reaction in swirling flow, *Scientific Reports*, 10, 2020, 7868.
[31] Atif, S.M., Hussain, S., Sagheer, M., Magnetohydrodynamic stratified bioconvective flow of micropolar nanofluid due to gyrotactic microorganisms, *AIP Advances*, 9(2), 2019, 025208-1-16.
[32] Khan, N.S., Shah, Q., Bhaumik, A., Kimam, P., Thounthong, P., Amiri, I., Entropy generation in bioconvection nanofluid flow between two stretchable rotating disks, *Scientific Reports*, 10, 2020, 1-26.
[33] Saleen, S., Rafiq, H., Qahatani, A.A., Aziz, M.A.E., Malik, M.Y., Animasaun, I.L., Magneto Jeffrey Nanofluid Bioconvection over a Rotating Vertical Cone due to Gyrotactic Microorganism, *Mathematical Problems in Engineering*, 2019, 2019, 3478037.
[34] Raju, C.S.K., Sandeep, N., Heat and mass transfer in MHD non-Newtonian bioconvection flow over a rotating cone/plate with cross diffusion, *Journal of Molecular Liquids*, 215, 2015, 115-126.
[35] Tarakaramu, N., Narayana, P.V.S., Chemical Reaction Effects on Bio-convection Nanofluid flow between two parallel plates in Rotating System with Variable Viscosity: A Numerical Study, *Journal of Applied and Computational Mechanics*, 5(4), 2019, 791-803.
[36] Siddheshwar, P.G., Kanchana, C., Unicellular unsteady Rayleigh-Benard convection in Newtonian liquids and Newtonian nanoliquids occupying enclosures: new findings, *International Journal of Mechanical Sciences*, 131-132, 2017, 1061-1072.
[37] Wakif, A., Boulahia, Z., Amine, A., Animasaun, I.L., Afridi, M.I., Qasimd, M., Sehaqui, R., Magneto-convection of alumina water nanofluid within thin horizontal layers using the revised generalised buongiorno's model, *Frontier in Heat and Mass Transfer*, 12(3), 2019, 1-15.
[38] Buongiorno, J., Convective Transport in Nanofluids, *Journal of Heat Transfer*, 128(3), 2006, 240-250.

[39] Nield, N.A., Kuznetsov, A.V., The onset of convection in a horizontal nanofluid layer of finite depth, *European Journal of Mechanics-B/Fluids*, 29(3), 2010, 217-223.
[40] Borujerdi, A.N., Noghrehabadi, A.R., Rees, D.A.S., Influence of Darcy number on the onset of convection in a porous layer with a uniform heat source, *International Journal of Thermal Sciences*, 47(8), 2008, 1020-1025.
[41] Nield, N.A., Kuznetsov, A.V., The Effect of Local Thermal Nonequilibrium on the Onset of Convection in a Nanofluid, *Journal of Heat Transfer*, 132(5), 2010, 052405-7.
[42] Yadav, D., Agarwal, G.S., Bhargava, R., Effect of Internal Heat Source on the Onset of Convection in a Nanofluid Layer, *Applied Mechanics and Materials*, 110-116, 2011, 1827-1832.
[43] Yadav, D., Bhargava, R., Magneto-convection in a rotating layer of nanofluid, *Asia-Pacific Journal of Chemical Engineering*, 9(5), 2014, 663-677.
[44] Chandrasekhar, S., *Hydrodynamic and Hydromagnetic Stability*, Oxford University Press, Oxford, 1961.

ORCID iD

Meenakshi Khurana https://orcid.org/0000-0003-0461-0108
Puneet Rana https://orcid.org/0000-0002-9850-763X

How to cite this article: Khurana M., Rana P., Srivastava S., Yadav S. Magneto-bio-thermal Convection in Rotating Nanoliquid containing Gyrotactic Microorganism, *J. Appl. Comput. Mech.*, 7(4), 2021, 1973–1986. https://doi.org/10.22055/JACM.2020.33456.2228